

Enhanced Spatial Resolution Scanning Kelvin Force Microscopy Using Conductive Carbon Nanotube Tips

Joseph J. Kopanski¹, Paul McClure², and Vladimir Mancevski²

¹*Semiconductor Electronics Division
National Institute of Standards and Technology
100 Bureau Dr., stop 8120
Gaithersburg, MD 20899*

²*Xidex Corporation
8906 Wall Street, Suite 703
Austin, Texas 78754*

Abstract. The response of a scanning Kelvin force microscope (SKFM) was measured with conventional micromachined silicon tips coated with Au and with advanced tips terminated with a carbon nanotube (CNT). A simple model of the SKFM predicts enhanced spatial resolution of the SKFM using a CNT terminated tip because it reduces the stray capacitance components due to the tip shank and the cantilever. SKFM measurements over abrupt boundaries between Au and silicon (with a thin silicon dioxide overlayer) show this predicted enhanced spatial resolution. The CNT-terminated tip resolves the boundary to less than a micrometer, while the conventional Au-coated tip smears the transition between the two materials over tens of micrometers.

Keywords: carbon nanotube, scanning Kelvin force microscope, SKFM, spatial resolution, work function

PACS: 68.37.Ps, 72.20.-I, 73.20.-r, 73.30.+y, 73.63.-b

INTRODUCTION

The scanning Kelvin force microscope (SKFM) is an interesting instrument with which to examine work function variations in a variety of materials and structures of interest for nanoelectronics. However, the amplitude modulated SKFM (am-SKFM) suffers from poor spatial resolution due to the capacitive coupling of all parts of the tip and cantilever to the sample [1]. The magnitude of the contribution to the total differential capacitive (dC/dz) signal of any element of the probe assembly varies with the inverse square of the distance between the element of the tip/cantilever and the sample. In operation, the am-SKFM cannot precisely locate abrupt boundaries between two materials with different work functions, and local measurements of work function are affected by the work function of the surrounding material. The spatial resolution of the SKFM can be enhanced via improved data acquisition techniques (i.e. frequency modulation [2-3]) and by using higher aspect ratio probe tips [4]. A simple model predicts that tips with high aspect

ratios and slightly blunt terminations will achieve better spatial resolution. In the extreme, this means that the ideal tip for a SKFM would be a cylinder. Carbon nanotube (CNT) tips mounted on the end of conventional micromachined silicon tips are close to this ideal shape. We have begun evaluating CNT tips for electrical scanning probe microscopy measurements on semiconductors and structures for integrated circuits. Areas of interest include two-dimensional dopant profiling, measurement of the work function of gate stack materials and of the tips themselves, measurement of dielectric constant for measuring damage to plasma etched low- κ dielectrics, measurement of strain-induced work function changes in semiconductors, and the use of the SKFM as a sensor for detecting work function changes in surfaces due to contaminants in the ambient atmosphere.

In the present study, we have compared CNT-terminated tips to conventional tips that are micro-machined from silicon and made conductive by coating with metal. Our simple model of the SKFM

was extended to include the effects of a terminal CNT tip. Both modeled and measured SKFM signals show substantial improvement in spatial resolution when using a CNT terminated tip as compared to the conventional SKFM tips.

CAPACITIVELY COUPLED SCANNING PROBE MICROSCOPES

The operation of the am-SKFM is described in detail elsewhere [1, 5-6]. Briefly, the am-SKFM uses a probe tip on a vibrating AFM cantilever to measure the contact potential difference (CPD) between the tip and the sample. As described by Coulomb's Law, there is an electrostatic force between two metal surfaces (the tip and sample) at different electrical potentials that is proportional to the differential capacitance; i.e. the change in capacitance with tip-sample distance (dC/dz). The electrical potential can be applied, or it can arise from the CPD between two metals with different work functions. An ac voltage is applied to the cantilever near its resonance frequency, and, as it changes the potential between the tip and sample, it changes the force on the cantilever driving it to oscillation. The am-SKFM adds a feedback loop between the tip and sample to find the dc voltage that minimizes the cantilever vibration. The voltage that minimizes the cantilever vibration is the voltage that exactly cancels the CPD between the tip and sample. In its simplest implementation, the SKFM utilizes an AFM in a double scan mode. In the first scan, the AFM measures topography. In the second scan, the tip is scanned over the surface topography offset by a constant distance from the surface. During this second scan, the SKFM feedback loop is activated, and the CPD profile is measured. Variations of the SKFM that measure both topography and CPD in a single scan mode have also been developed [7].

While the atomic force microscope can achieve remarkable spatial resolution (to the atomic level), any scanning probe technique that depends directly on the variation of the capacitance with tip-to-sample distance is subject to large stray capacitance effects. AFM depends on the van der Waals force, which varies as the inverse seventh power of the probe to space spacing, while am-SKFM depends on the electric field, which varies with the inverse square of the spacing between electrodes. Because the tip in the vicinity of the sample has a small area relative to the rest of the probe tip assembly, the shank of the probe and even the cantilever contribute significant components of the total capacitance affecting the SKFM, even though they are farther from the sample.

Previously [1], we introduced a simple model that allowed the contributions of the tip, tip shank, and cantilever to the total differential capacitance affecting the SKFM to be estimated. The magnitudes of these dC/dz components, for a commercially available tip useful for SKFM, are plotted versus tip-to-sample separation in Figure 1. The simulated tip is modeled as a terminal spherical tip with a radius of 20 nm, a conical tip shank with a cone angle of 28 degrees and a height of 20 μm , and a cantilever with a length of 125 μm and a width of 35 μm . Note that as tip lift height is increased above a few nanometers, the contributions to dC/dz due to the shank and the cantilever rapidly come to dominate the total capacitance. This tip has a relatively long shank (20 μm), minimizing the effect of the cantilever. However, the wide cone angle of the shank results in a substantial contribution to the local measured CPD. Results from this model emphasize that the ideal shape of a SKFM tip is a nearly cylindrical tip shank. A long shank serves to isolate the contribution to the SKFM signal from the small area terminal tip, which is nearly in contact with the surface, from the much larger area cantilever capacitance.

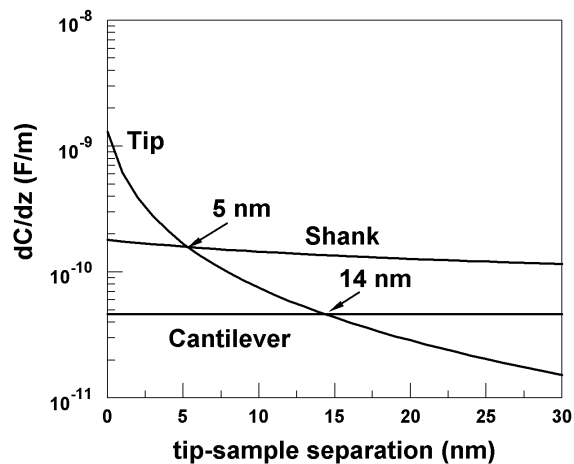


FIGURE 1. Differential capacitance (dC/dz) of the elements of a typical micromachined, Au-coated, silicon cantilevered tip useful for SKFM as a function of tip lift height. Here the tip is modeled as a sphere, the shank as a cone, and the cantilever as a series of planar elements. At a tip-sample separation of 5 nm, the dC/dz of the shank exceeds that of the tip; at 14 nm, the dC/dz of the cantilever exceeds that of the tip.

CNT terminated tips can simulate this ideal tip shape. A Scanning Electron Microscope (SEM) photograph of the tip used in the measurements reported here is shown as Figure 2. Here a relatively short CNT (225 nm) terminates a micromachined silicon tip shank a number of micrometers long. By offsetting the tip shank from the surface, the relative

contribution of the shank to total SKFM dC/dz is significantly attenuated relative to the contribution of the terminal tip. Figure 3 shows the effect on dC/dz of adding modest length (225 nm and 500 nm) CNTs to the end of the tip. Here the tip is also modeled as sphere with a 20 nm radius, but the other components to dC/dz are offset by the CNT length. Offsetting the bulk of the tip shank from the CNT terminal tip by 225 nm reduces the contribution of the shank by a factor of about 3; offsetting by 500 nm reduces the shank contribution by a factor of 6. The ratio of the contribution to dC/dz from the CNT tip to that from the shank is plotted versus CNT length in Figure 4. For this geometry, CNT tips longer than 1.3 μm reduce the contribution due to the tip shank to less than a few percent. The contribution to dC/dz due to the cantilever is less dramatically affected by the addition of a CNT as the cantilever starts offset by the tip shank cone length (20 μm in this example).

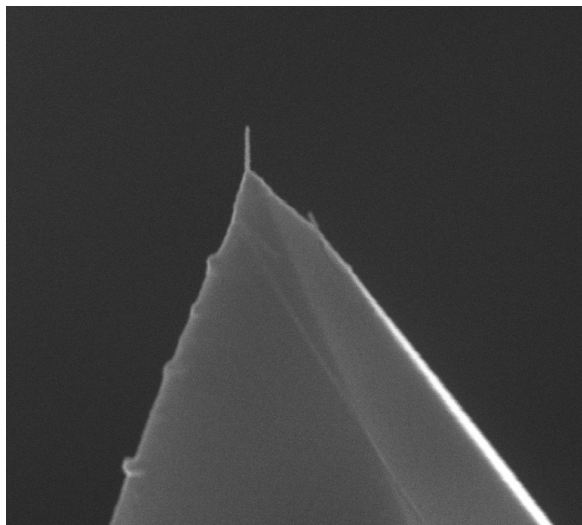


FIGURE 2. SEM micrograph of the CNT terminated tip used in these measurements. CNT tip length is approximately 225 nm. Tips are fabricated using a proprietary process by Xidex Inc.*

CONTACT POTENTIAL DIFFERENCE ACROSS AN ABRUPT BOUNDARY

To determine the effect on SKFM spatial resolution of CNT terminated tips, we simulated and measured the SKFM signal across an abrupt boundary in work function. The simulated structure was an abrupt

*Certain commercial equipment, instruments, or materials are identified in this paper in order to specify adequately the experimental procedure. Such identification does not imply recommendation or endorsement by NIST, nor does it imply that the materials or equipment used are necessarily the best available for the purpose.

boundary between Au and silicon (covered with a 5 nm oxide). The simulated tips were an Au-coated tip, like that simulated in Fig. 1, and a similar tip terminated by a 225 nm CNT. Simulated work functions were $\phi_{\text{Au}} = 5.1$ eV, $\phi_{\text{Si}} = 4.8$ eV, and

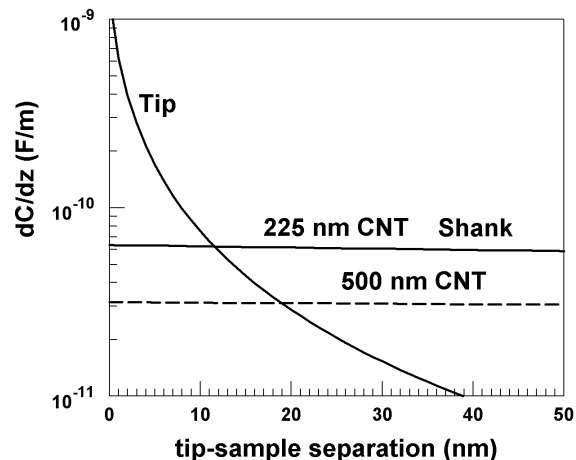


FIGURE 3. Differential capacitance (dC/dz) of the elements of an advanced CNT terminated tip useful for the SKFM. The geometry of this tip is identical to the tip shown in Fig. 1, except for the addition of terminal CNTs with a length of either 225 nm or 500 nm. For comparison purposes, the radius of the CNT was simulated as the same as the Au-coated tip in Fig. 1 (20 nm). The contribution of the CNT tip to the total dC/dz is dominant for tip-sample separations less than 12 μm .

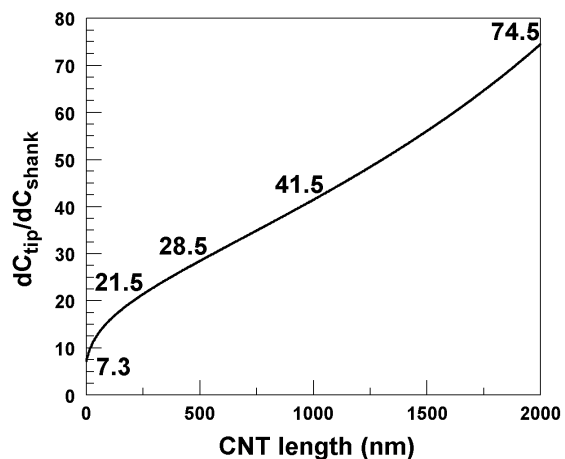


FIGURE 4. Ratio of dC/dz for a 20 nm terminal CNT tip to the dC/dz of a conical tip with a cone angle of 28 degrees. Contribution of the shank is reduced to less than 2% of the tip for a CNT length of 1.3 μm .

$\phi_{\text{CNT}} = 5.4$ eV. The value used for the work function of the oxidized silicon is based on the work function of Si with a small potential drop across the thin oxide. The value for the CNT is estimated from measurements of CPD using this tip and metals of known work functions. This model simply considers geometric

effects and does not account for more detailed physics, such as the band bending at the interface or electric field spreading in three dimensions. Figure 5 shows the result of this simulation. Here, the silicon is to the left and the Au to the right, with the 0 μm tip position corresponding to the point where the center of the terminal tip is at the abrupt boundary. As expected, the CPD measured with the CNT tip is 0.3 eV higher than with the Au-coated tip. In these simulations, the shank produces a blurring of the abrupt boundary by approximately the width of the shank at the cantilever height (around 11 μm for this tip simulation geometry). The addition of the CNT to the tip greatly attenuates the contribution of the shank to the measured CPD profile. While this model qualitatively reproduces the effect of the different components of tip shape on the CPD, only rough agreement with individual tips is expected without knowing the actual tip parameters in more detail.

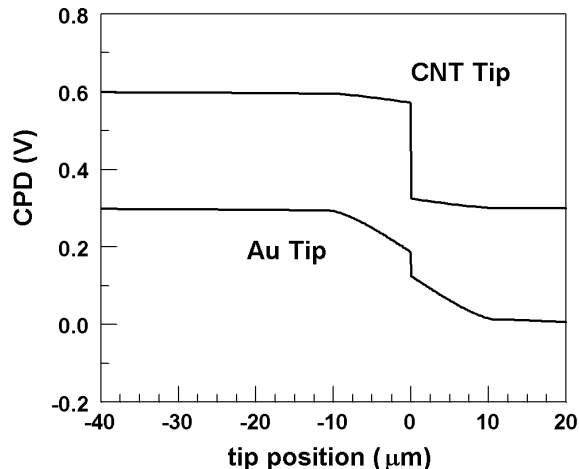


FIGURE 5. Modeled CPD profile that would be measured with SKFM for an abrupt boundary between Au and Si. The Au-coated tip shows substantial smearing of the boundary between Au and Si, while the 225 nm CNT-terminated tip resolves the boundary more precisely. Both tips have the same radius. The offset in CPD is due to the different work functions of the Au tip and the CNT tip.

CPD profiles measured with real tips across an Au-pad to silicon boundary are shown in Figure 6. The CNT tip defines the boundary in CPD much more precisely than the Au-coated tip. For the CNT-terminated tip, the transition in measured CPD is confined to a region of no more than a few micrometers at the actual metal-silicon boundary. For the Au-coated tip, a transition is seen at the metal-silicon boundary, but the CPD never reaches a constant value, even when the tip is 40 μm from the boundary. This is because the tip shank contributes a large component to the total dC/dz over a region extending 10 μm to either side of the boundary. An

additional contribution to dC/dz due the cantilever smears the apparent transition even more.

The actual width of the transition is difficult to determine for this sample because of non-ideal topography. The Au layer was sputter-deposited, and the pad was defined by lift-off lithography. The Au film thickness was approximately 20 nm and had a topographic feature at the boundary. This “lip” at the metal pad edge was an artifact of the lift-off process used to define the Au pad and affected the measured CPD, showing up as an apparent spike in the CPD. Since the SKFM measures CPD, topographic features should not affect the CPD signal. The presence of the topographic feature in the CPD profile may be due to an effective change in the tip area as the tip shank contacts the lip, or it may be due to a disturbance in the SKFM feedback loop. Comparing our simulations to experimental results, we found that the CPD profile experimentally measured with the CNT was even sharper than predicted by the model. We attribute this to the relatively lower sticking coefficient of the hydrophobic CNT tip as compared to the Au tip. Because of this, the CNT tips may actually be operating closer to the actual surface than the Au-coated tips, further enhancing the contribution of the terminal tip to the total dC/dz . Note also that the CPD measured with the CNT picks up additional fine features in the CPD. These features repeat from scan-to-scan and contribute coherent structure to the SKFM image of the CPD. Hence, it is clear that the additional structure is not due to a higher noise level, but due to actual short scale variations in apparent CPD.

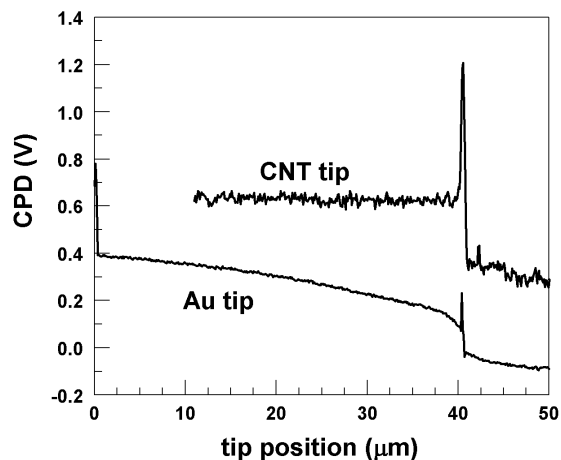


FIGURE 6. SKFM measured CPD profile for an abrupt boundary between an Au pad and Si with a 5 nm oxide overlayer. The boundary is near the 40 μm point of these scans. The Au-coated tip shows substantial smearing of the boundary between Au and Si, while the CNT-terminated tip resolves the boundary more precisely. The spike at the boundary is related to the Au pad topography.

CONCLUSIONS

CNT-terminated tips promise an easy way of enhancing the spatial resolution of the am-SKFM for work function measurements. A simple model of the SKFM predicts that a relatively short CNT will reduce the effect of the tip shank and improve the spatial resolution of the am-SKFM. This effect was apparent in both simulations and measurements with a 225 nm CNT-terminated SKFM tip. Experimentally, SKFM measurements using the CNT-terminated tip resolve an abrupt boundary between two materials with different work functions to less than a micrometer, while the conventional Au-coated tip smears the transition between the two materials over tens of micrometers. Simulations predict that, for this tip geometry, CNT tips of 1.3 μm will reduce the shank contribution to the measured CPD to less than 2 % of that of the tip. The actual optimal length of the CNT tip will depend on the cone angle and length of the shank to which it is attached. The CNT also reduces the contribution to total dC/dz of the cantilever, but not as dramatically as the cantilever is already offset from the surface by the shank length. The lower sticking coefficient of the hydrophobic CNT tip may also help improve spatial resolution by allowing smaller lift heights to be maintained.

ACKNOWLEDGMENTS

The authors thank Victor Vartanian of the International Sematech Manufacturing Initiative (ISMI), Albany, NY, for introducing them and suggesting this project. This work was supported by the Office of Microelectronics Programs, National Institute of Standards and Technology.

REFERENCES

1. J. J. Kopanski, M. Y. Afridi, S. Jelazkov, W. Jiang, and T. R. Walker, AIP Conference Pro. **CP931**, *Frontiers of Characterization and Metrology for Nanoelectronics*, p. 530-534 (American Institute of Physics, 2007).
2. U. Zerweck, C. Loppacher, T. Otto, S. Grafström, and L. M. Eng, *Phys. Rev. B* **71**, 125424 (2005).
3. C. Loppacher, U. Zerweck, S. Teich, E. Beyreuther, T. Otto, S. Grafström, and L. M. Eng, *Nanotechnology* **16**, S1-S6 (2005).
4. M. Zhao, V. Sharma, H. Wei, R. R. Birge, J. A. Stuart, F. Papadimitrakopoulos, and B. D. Huey, *Nanotechnology* **19**, 235704-10 (2008).
5. M. Nonenmacher, M. P. O'Boyle, and H. K. Wickramasinghe, *Appl. Phys. Lett.* **58**, 2921-2923 (1991).
6. S. Sadewasser and M. C. Lux-Steiner, *Phys. Rev. Lett.* **91**, 266101 (2003).

7. D. Ziegler, J. Rychen, N. Naujoks, and A. Stemmer, *Nanotechnology* **18**, 225505 (2007).